

# Integral High Order Sliding Mode Control of a Brake System

Juan Diego Sánchez-Torres<sup>†</sup>, Antonio Navarrete-Guzmán<sup>‡</sup> and Alexander G. Loukianov<sup>§</sup>  
Department of Electrical Engineering and Computer Science,  
Automatic Control Laboratory,  
CINVESTAV Unidad Guadalajara, Zapopan, Jalisco, 45015 México.  
<sup>†</sup>dsanchez@gdl.cinvestav.mx, <sup>‡</sup>anavarret@gdl.cinvestav.mx, <sup>§</sup>louk@gdl.cinvestav.mx

**Abstract**—The aim of this paper is to present the design of a robust sliding mode control scheme for a vehicle system which consists of active brake systems. The proposed control strategy is based on the combination of high order sliding mode control methods and integral sliding mode control, taking advantage of the block control principle. The brake controller induces the antilock brake system feature by means of tracking the slip rate of the car, improving the stability in the braking process and preventing the vehicle from skidding.

**Index Terms:** Antilock braking systems, Automotive control, Sliding mode control, Integral control

## I. INTRODUCTION

One of the most important control objectives in automotive systems is to provide adequate safety and to keep the vehicle occupants comfortable. An example is the controller design for the brake system. The wheel skidding is an undesirable phenomena which often results when the wheels get locked, leading to lose control of the car. Therefore, it is necessary to design brake controllers that induce the anti-lock brake system (ABS), preventing wheels from locking up during hard braking (Petrov *et al.*, 1977; Rittmannsberger, 1988; Emig *et al.*, 1990).

For many drivers the ABS usually offers improved vehicle control and decreases stopping distances on dry and slippery surfaces. In contrast, ABS can significantly increase braking distance on loose surfaces like gravel or snow-covered pavement, although still improving vehicle control (Burton *et al.*, 2004). Generally, the ABS design is based on the idea of reducing the pressure on the brake cylinder when the wheel is close to lock. This is done until the wheel velocity exceeds some threshold value. This breaking process may be improved by regulating the wheel slip (Tan and Chin, 1991). Thus, modern ABS systems not only try to prevent wheels from locking but also try to maximize the breaking forces generated by the tires to prevent that the longitudinal slip ratio exceeds an optimal value (Rajamani, 2011).

The main difficulties arising in the controller design for the brake system are due to uncertainties and the high nonlinearity presented in the system model. Therefore, the ABS has become an attractive examples for research in area of robust control. As proposals, several works have been

applied the sliding mode (SM) technique to design a slip-ratio controller for the vehicle stability; some examples are (Tan and Chin, 1991; Unsal and Pushkin, 1999; Ming-Chin and Ming-Chang, 2003; Tanelli *et al.*, 2009; Delprat and Ferreira de Loza, 2011), including the extremum seeking controllers in order to maximize the friction between the tire and the road (Chin *et al.*, 1992; Drakunov *et al.*, 1995; Tunay, 2001).

In this paper, the main purpose is to propose an ABS controller in presence of external disturbances and parametric variations, which are supposed to be unknown but bounded. The solution for the exposed problem is based on SM algorithms. These algorithms are proposed with the idea to drive the dynamics of a system to a sliding manifold, that is an integral manifold with finite reaching time (Drakunov and Utkin, 1992); exhibiting features such as SM motion finite time convergence, robustness to uncertainties including plant parameter variations and external bounded disturbances (Utkin *et al.*, 2009). To design the brake controller, a combination of block control feedback linearization (Loukianov, 2002), integral SM control (Utkin *et al.*, 2009) and high order quasi-continuous SM algorithms (Levant, 2005) is used in order to obtain an exact rejection of the system disturbances, similarly to the method shown by (Estrada and Fridman, 2010). The integral SM control methods guarantee the robustness of the closed-loop system throughout the entire response starting from the initial time instant, and reduces the sliding functions gains in comparison with the standard SM control. This approach is based on the integral nested SM control technique (Huerta-Avila *et al.*, 2007), which combines the integral SM control (Utkin *et al.*, 2009) with the nested SM control (Adhami-Mirhosseini and Yazdanpanah, 2005) and, has been applied for the ABS design as shown in (Sánchez-Torres *et al.*, 2013), bounding the effect of disturbances to an arbitrary small vicinity of zero, however without exact rejection.

The work is organized as follows: The mathematical model for the brake system is presented in Section II. Section III exposes the design of the SM controllers for the brake, with special emphasis in the sliding manifold design. The simulation results are presented in Section IV,

verifying the performance of the proposed control strategy. Finally, the conclusions are presented in Section V.

## II. MATHEMATICAL MODEL

In this section, the dynamic equations which represent brake system, are presented. This system consider a quarter of the vehicle model and includes the dynamics of pneumatic brake system, wheel and vehicle.

### A. Pneumatic Brake System Equation

The specific configuration of this system model considers the brake disk system. The brake holds the wheel, as a result of the air pressure increment in the brake cylinder. The air entrance trough the pipes from the central reservoir and the air expulsion from the brake cylinder to the atmosphere, are regulated by a common valve.

Considering Figure 1, the brake torque  $T_b$  is supposed to be proportional to the pressure  $P_b$  in the brake cylinder

$$T_b = k_b P_b \quad (1)$$

with  $k_b > 0$ . For the brake system, an approximated first order model of pressure changes in the brake cylinder due to the opening of the valve, is applied (Clover and Bernard, 1998):

$$\tau \dot{P}_b + P_b = P_c \quad (2)$$

where  $P_c$  is the pressure inside the central reservoir, and  $\tau$  is the time constant of the pipelines. The atmospheric pressure,  $P_a$ , is considered as equal to zero.

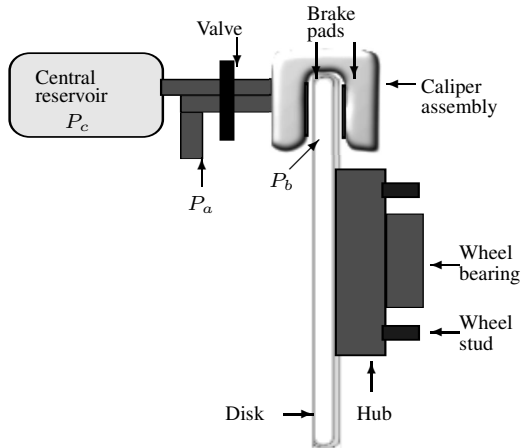


Fig. 1. Pneumatic brake scheme

### B. Wheel Motion Equations

To describe the wheel motion, the mathematical model derived in (Kruchinin *et al.*, 2001) is used.

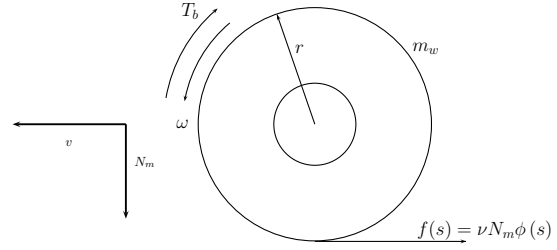


Fig. 2. Active suspension and wheel forces and torques

Considering Figure 2, the dynamics of the angular momentum variation relative to the rotation axis, are represented by

$$J\dot{\omega} = r f(s) - b_b \omega - T_b \quad (3)$$

where  $\omega$  is the wheel angular velocity,  $J$  is the wheel inertia moment,  $r$  is the wheel radius,  $b_b$  is a viscous friction coefficient due to wheel bearings,  $f(s)$  is the contact force of the wheel and  $s$  is the slip rate.

The expression for the longitudinal component of the contact force in the motion plane is

$$f(s) = \nu N_m \phi(s) \quad (4)$$

where  $\nu$  is the nominal friction coefficient between the wheel and the road,  $N_m$  is the normal reaction force in the wheel and it is defined by  $N_m = mg$ , with  $g$  the gravity acceleration and  $m$  the mass supported by the wheel.

The function  $\phi(s)$  represents the longitudinal friction/slip characteristic relation between the tire and road surface. In general, its calculation is based on experimental tests (Bakker *et al.*, 1987). A plot of this function for different surfaces is shown in Figure 3.

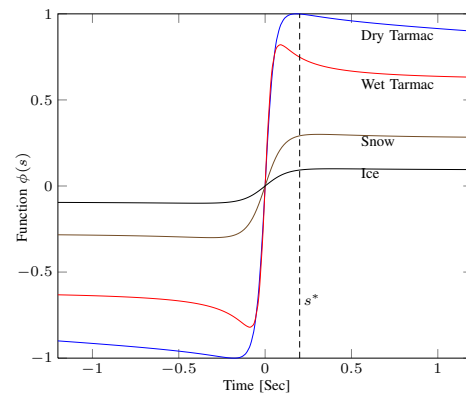


Fig. 3. Characteristic function  $\phi(s)$

To approximate the function  $\phi(s)$ , the Pacejka formula (Bakker *et al.*, 1987) is used. This model is defined as follows:

$$\phi(s) = D \sin(C \arctan(Bs - E(Bs - \arctan(Bs))))$$

where  $B$ ,  $C$ ,  $D$  and  $E$  are the model parameters which are adjusted by using experimental data.

Based on the mentioned experimental tests, the Pacejka formula produces a good approximation of the tire/road friction interface, fitting accurately the data obtained via measurement of the road conditions (Pacejka, 1981; Bakker *et al.*, 1989; Pacejka, 2012). Table I shows the estimated parameters for different road conditions.

Surface	B	C	D	E
Dry Tarmac	10	1.9	1	0.97
Wet Tarmac	12	2.3	0.82	1
Snow	5	2	0.30	1
Ice	4	2	0.10	1

TABLE I

PACEJKA MODEL PARAMETERS FOR DIFFERENT ROAD SURFACES.

The slip rate  $s$  is defined as

$$s = \frac{v - r\omega}{v} \quad (5)$$

where  $v$  is the longitudinal velocity of the wheel mass center. For  $s > 0$ , the function  $\phi(s)$  represents braking conditions. In Figure 3,  $s^*$  represents the desired value for the slip rate  $s$ . A suitable choice of  $s^*$  is value in the small interval  $0.15 \leq s^* \leq 0.25$ , this selection ensures a high longitudinal friction for the different road conditions.

The equations (3)-(5) characterize the wheel motion.

### C. The Vehicle Motion Equation

The vehicle longitudinal dynamics considered without lateral motion, are described by

$$M\dot{v} = -F(s) - F_a(v, t) \quad (6)$$

where  $M$  is the total vehicle mass,  $F_a$  is the aerodynamic drag force which is proportional to the vehicle velocity. This force is defined as

$$F_a(v, t) = \frac{1}{2}\rho C_d A_f (v + v_w(t))^2$$

where  $\rho$  is the air density,  $C_d$  is the aerodynamic coefficient,  $A_f$  is the frontal area of vehicle,  $v_w$  is the wind velocity, and the contact force of the vehicle  $F(s)$  is modeled of the form

$$F(s) = \nu N_M \phi(s) \quad (7)$$

where  $N_M$  is the normal reaction force of the vehicle, defined as  $N_M = Mg$ .

### D. State Space Equations

The complete system (2)-(6), using the state variables  $\mathbf{x} = [x_1 \ x_2 \ x_3]^T = [\omega \ P_b \ v]^T$ , is presented in the following form:

$$\begin{aligned} \dot{x}_1 &= -a_1 x_1 + a_2 f(s) - a_3 x_2 \\ \dot{x}_2 &= -a_4 x_2 + bu \\ \dot{x}_3 &= -a_5 F(s) - a_5 F_a(x_3, t) \end{aligned} \quad (8)$$

with the output

$$y = x_1 \quad (9)$$

where  $a_1 = b_b/J$ ,  $a_2 = r/J$ ,  $a_3 = k_b/J$ ,  $a_4 = 1/\tau$ ,  $a_5 = 1/M$ ,  $b = 1/\tau$ ,  $u = P_c$ .

## III. CONTROLLER DESIGN

The task of controlling the wheels rotation is studied in this section. The controller is designed such that the longitudinal force due to the contact of the wheel with the road, is near to the maximum value in the time period valid for the model. This maximum value is reached as a result of the brake valve effort (see Figure 1).

Considering the direct action of the pressure  $P_b$  in the brake cylinder over the wheel, the output tracking error

$$e_1 = x_1 - \frac{1 - s^*}{r} x_3. \quad (10)$$

is defined.

From (8) and (10), with the variables  $x_1$  and  $x_3$  written in terms of  $e_1$ , it follows that

$$\dot{e}_1 = f_1(e_1) + b_1 x_2 + \Delta_1(\mathbf{x}, t) \quad (11)$$

where  $f_1(e_1) = \left[ a_2 N_m + \frac{1-s^*}{r} a_5 N_M \right] \nu \phi(s) - a_1 x_1$  and  $b_1 = -a_3$ . The disturbance term  $\Delta_1(\mathbf{x}, t)$  in (11) contains the unknown aerodynamic drag force  $-\frac{1-s^*}{r} a_5 F_a(x_3, t)$ , the reference derivative  $\dot{s}^*$  and, the variations of the friction parameter  $\nu$ . In the control design, the term  $\Delta_1(\mathbf{x}, t)$  will be considered as a bounded disturbance.

To stabilize the dynamics for  $e_1$  in (11),  $x_2$  can be selected as a stabilizing term in form of a virtual controller, the desired value for  $x_2$ ,  $x_{2des}$  is determined as

$$x_{2des} = x_{2des}^0 + x_{2des}^1 \quad (12)$$

where  $x_{2des}^1$  will be designed to reject the disturbance  $\Delta_1(\mathbf{x}, t)$  in finite time by using the integral sliding mode technique (Utkin *et al.*, 2009) in combination quasi-continuous SM control (Levant, 2005). The term  $x_{2des}^0$  is such that  $e_1$  converges exponentially to zero.

In order to establish the control  $x_{2des}$  in (11), the error variable  $e_2$  is defined as

$$e_2 = x_2 - x_{2des} \quad (13)$$

and (11) is rewritten as

$$\dot{e}_1 = f_1(e_1) + b_1 e_2 + b_1 x_{2des} + \Delta_1(\mathbf{x}, t). \quad (14)$$

To calculate the term  $x_{2des}^1$ , the variable  $\sigma_1$  is proposed as

$$\sigma_1 = e_1 + z_1 \quad (15)$$

where  $z_1$  is a SM integral variable to be defined below.

From (11) and (15), the dynamics for  $\sigma_1$  are given by

$$\begin{aligned} \dot{\sigma}_1 &= f_1(e_1) + b_1 x_{2des}^0 + b_1 x_{2des}^1 + b_1 e_2 \\ &\quad + \Delta_1(\mathbf{x}, t) + \dot{z}_1 \end{aligned} \quad (16)$$

where the derivative  $\dot{z}_1$  is assigned of the form

$$\dot{z}_1 = -f_1(e_1) - b_1 x_{2des}^0 \quad (17)$$

with  $z_1(0) = -e_1(0)$  in order to fulfill the requirement  $\sigma_1(0) = 0$ . With this selection of  $\dot{z}_1$ , the system (16) reduces to

$$\dot{\sigma}_1 = b_1 x_{2des}^1 + b_1 e_2 + \Delta_1(\mathbf{x}, t). \quad (18)$$

To enforce sliding motion on the manifold  $\sigma_1 = 0$  despite of the disturbance  $\Delta_1(\mathbf{x}, t)$ , the term  $x_{2des}^1$  in (18) is chosen as

$$x_{2des}^1 = b_1^{-1} \xi \quad (19)$$

with  $\xi$  the solution of

$$\dot{\xi} = -\alpha \frac{\dot{\sigma}_1 + \beta |\sigma_1|^{\frac{1}{2}} \text{sign}(\sigma_1)}{|\dot{\sigma}_1| + \beta |\sigma_1|^{\frac{1}{2}}} \quad (20)$$

where  $\alpha > 0$  and  $\beta > 0$ .

When the motion on the manifold  $\sigma_1 = 0$  is reached, the solution of  $\dot{\sigma}_1 = 0$  in (16)

$$b_1 \{x_{2des}^1\}_{eq} = \Delta_1(\mathbf{x}, t). \quad (21)$$

shows that the disturbance  $\Delta_1(\mathbf{x}, t)$  is rejected by the equivalent control  $b_1 \{x_{2des}^1\}_{eq}$  (Utkin, 1992). Therefore, the dynamics on  $\sigma_1 = 0$  is given by

$$\dot{e}_1 = f_1(e_1) + b_1 x_{2des}^0. \quad (22)$$

Thus, the desired dynamics  $-k_1 e_1$  for  $\dot{e}_1$  in (22) are introduced by means of

$$x_{2des}^0 = b_1^{-1} [-f_1(e_1) - k_1 e_1] \quad (23)$$

where  $k_1 > 0$ . Hence, with (23) in (17),  $\dot{z}_1$  reduces to

$$\dot{z}_1 = k_1 e_1. \quad (24)$$

From (13), it follows that

$$\dot{e}_2 = bu - \Delta_2(\mathbf{x}, t) \quad (25)$$

where the term  $\Delta_2(\mathbf{x}, t) = \dot{x}_{2des}$  is a bounded disturbance.

Considering the types of valve that can vary its position in a continuous range, the integral SM control method is applied to (25) in order to induce a sliding mode on the manifold  $e_2 = 0$  in spite of the disturbance  $\Delta_2(\mathbf{x}, t)$ . With this aim, the control  $u$  is decomposed as

$$u = u_0 + u_1 \quad (26)$$

where  $u_1$  will reject the disturbance  $\Delta_2(\mathbf{x}, t)$  in finite time and  $u_0$  is designed to stabilize  $e_2$  in finite time.

To calculate the term  $u_1$ , the variable  $\sigma_2$  is proposed as

$$\sigma_2 = e_2 + z_2 \quad (27)$$

where  $z_2$  is a SM integral and it will be defined below.

Considering the equations (25) and (27), the dynamics for  $\sigma_2$  are given by

$$\dot{\sigma}_2 = bu_0 + bu_1 - \Delta_2(\mathbf{x}, t) + \dot{z}_2. \quad (28)$$

Selecting  $\dot{z}_2$  as

$$\dot{z}_2 = -bu_0 \quad (29)$$

the system (28) reduces to

$$\dot{\sigma}_2 = bu_1 - \Delta_2(\mathbf{x}, t). \quad (30)$$

To enforce sliding motion on the manifold  $\sigma_2 = 0$  despite of the disturbance  $\Delta_2(\mathbf{x}, t)$ , the term  $u_1$  in (30) is chosen as the *super-twisting* algorithm (Levant, 1993)

$$u_1 = b^{-1}(u_{11} + u_{12}) \quad (31)$$

where  $u_{11} = -k_{11} |\sigma_2|^{\frac{1}{2}} \text{sign}(\sigma_2)$  and  $\dot{u}_{12} = -k_{12} \text{sign}(\sigma_2)$ , with  $k_{11} > 0$  and  $k_{12} > 0$ .

On the manifold  $\sigma_2 = 0$ , the solution of  $\dot{\sigma}_2 = 0$  in (28) leads to

$$b \{u_1\}_{eq} = \Delta_2(\mathbf{x}, t). \quad (32)$$

showing that the disturbance  $\Delta_2(\mathbf{x}, t)$  is rejected by the equivalent control  $b \{u_1\}_{eq}$  (Utkin, 1992). Thus, the dynamics for  $e_2 = 0$  is given by

$$\dot{e}_2 = bu_0. \quad (33)$$

Finally, the desired dynamics for  $\dot{e}_2$  in (33) are introduced with

$$u_0 = -k_2 b^{-1} |e_2|^{\frac{1}{2}} \text{sign}(e_2) \quad (34)$$

where  $k_2 > 0$ . Thus, with (34) in (29),  $\dot{z}_2$  yields to

$$\dot{z}_2 = k_2 |e_2|^{\frac{1}{2}} \text{sign}(e_2). \quad (35)$$

Using the nonsingular transformation (10), (13), (19) and (23)

$$\begin{aligned} e_1 &= x_1 - \frac{1-s^*}{r} x_3 \\ e_2 &= x_2 + b_1^{-1} [-f_1(e_1) - k_1 e_1] + b_1^{-1} \xi \\ \sigma_1 &= e_1 + z_1 \\ \sigma_2 &= e_2 + z_2 \end{aligned}$$

with the integral variables  $z_1$ ,  $z_2$  and  $\xi$  defined by (24), (35) and (20), respectively; the extended closed loop system (11) and (25) is presented as

$$\begin{cases} \dot{e}_1 &= -k_1 e_1 + \xi + b_1 e_2 + \Delta_1(\mathbf{x}, t) \end{cases} \quad (36)$$

$$\begin{cases} \dot{\sigma}_1 &= \xi + b_1 e_2 + \Delta_1(\mathbf{x}, t) \\ \dot{\xi} &= -\alpha \frac{\dot{\sigma}_1 + \beta |\sigma_1|^{\frac{1}{2}} \text{sign}(\sigma_1)}{|\dot{\sigma}_1| + \beta |\sigma_1|^{\frac{1}{2}}} \end{cases} \quad (37)$$

$$\begin{cases} \dot{e}_2 &= -k_2 |e_2|^{\frac{1}{2}} \text{sign}(e_2) - k_{11} |\sigma_2|^{\frac{1}{2}} \text{sign}(\sigma_2) \\ &+ \dot{u}_{12} + \Delta_2(\mathbf{x}, t) \end{cases} \quad (38)$$

$$\begin{cases} \dot{\sigma}_2 &= -k_{11} |\sigma_2|^{\frac{1}{2}} \text{sign}(\sigma_2) + u_{12} + \Delta_2(\mathbf{x}, t) \\ \dot{u}_{12} &= -k_{12} \text{sign}(\sigma_2). \end{cases} \quad (39)$$

Considering the disturbances in the closed-loop system (36) - (39) as fulfilling the following conditions:

$$\left| \dot{\Delta}_1(\mathbf{x}, t) \right| \leq L_1 \quad (40)$$

$$\left| \dot{\Delta}_2(\mathbf{x}, t) \right| \leq L_2 \quad (41)$$

in some admissible region  $\Omega_0$  with  $L_1 > 0$  and  $L_2 > 0$ , the stability of the closed-loop system (36) - (39) is outlined in the stepwise procedure

**Step A)** The SM stability of the projection motion (39).

**Step B)** Reaching phase of the projection motion (38).

**Step C)** The SM stability of the projection motion (37).

**Step D)** The SM motion stability of (36) on the manifold  $e_2 = 0$ .

**Step A)** Using the transformation  $q = u_{12} + \Delta_2(\mathbf{x}, t)$ , the system (39) yields to

$$\begin{aligned}\dot{\sigma}_2 &= -k_{11}|\sigma_2|^{\frac{1}{2}}\text{sign}(\sigma_2) + q \\ \dot{q} &= -k_{12}\text{sign}(\sigma_2) + \dot{\Delta}_2(\mathbf{x}, t).\end{aligned}\quad (42)$$

Under the assumption (41), it follows that if  $k_{11} > 0$  and  $k_{22} > 3L_2 + 4\left(\frac{L_2}{k_{11}}\right)^2$ , then  $(\sigma_2, q) = (0, 0)$  in finite time despite of the perturbation  $\Delta_2(\mathbf{x}, t)$  (Moreno and Osorio, 2008).

**Step B)** In (38), the motion on the manifold  $\sigma_2 = 0$  is given by

$$\dot{e}_2 = -k_2|e_2|^{\frac{1}{2}}\text{sign}(e_2).\quad (43)$$

Let the Lyapunov candidate  $V = \frac{1}{2}e_2^2$ . From (43), it follows

$$\dot{V} = -k_2 2^{\frac{3}{4}} V^{\frac{3}{4}}.\quad (44)$$

Therefore,  $e_2$  converges to zero in finite time; establishing a SM in the manifold  $e_2 = 0$ .

**Step C)** For (37), the motion on the manifold  $e_2 = 0$  is given by

$$\begin{aligned}\dot{\sigma}_1 &= \xi + \Delta_1(\mathbf{x}, t) \\ \dot{\xi} &= -\alpha \frac{\dot{\sigma}_1 + \beta |\sigma_1|^{\frac{1}{2}}\text{sign}(\sigma_1)}{|\dot{\sigma}_1| + \beta |\sigma_1|^{\frac{1}{2}}}\end{aligned}\quad (45)$$

With the transformation  $\varphi_1 = \sigma_1$  and  $\varphi_2 = \dot{\sigma}_1$ , the system (45) is written as

$$\begin{aligned}\dot{\varphi}_1 &= \varphi_2 \\ \dot{\varphi}_2 &= -\alpha \frac{\varphi_2 + \beta |\varphi_1|^{\frac{1}{2}}\text{sign}(\varphi_1)}{|\varphi_2| + \beta |\varphi_1|^{\frac{1}{2}}} + \dot{\Delta}_1(\mathbf{x}, t).\end{aligned}\quad (46)$$

Under the condition (40), there exist  $\alpha > 0$  and  $\beta > 0$  such that the system (46) is finite time stable (Levant, 2005), i.e., its solution converges in finite time to the origin  $(\varphi_1, \varphi_2) = (\sigma_1, \dot{\sigma}_1) = (0, 0)$ , inducing a SM on  $\sigma_1 = 0$ .

**Step D)** The motion for (36) on the set  $(e_2, \sigma_1) = (0, 0)$  is given by the system

$$\dot{e}_1 = -k_1 e_1\quad (47)$$

which is exponentially stable.

Note that during the braking process  $x_3 > 0$  and with  $s \approx s^*$ , due to the control action, the dynamics for  $x_3$  becomes

$$\dot{x}_3 = -a_5 F(s^*) - a_5 F_a(x_3, t).\quad (48)$$

From the vehicle mechanics, the term  $a_5 F_a(x_3, t)$  can be considered to be bounded  $|a_5 F_a(x_3, t)| \leq \delta_3$ , with  $\delta_3 > 0$ . In addition, it can be considered that  $a_{11} F(s^*) \gg \delta_7$ .

Therefore, let  $\gamma = a_{11} F(s^*) - \delta_7$ , and  $W = \frac{1}{2}x_3^2$ , then  $\dot{W} = -x_3 [a_5 F(s^*) + a_5 F_a(x_3, t)] < -\gamma x_3$ . Hence,  $\dot{W} < -\gamma_0 \sqrt{W}$ , where  $\gamma_0 = \gamma \sqrt{2}$ . Thus,  $x_3 = 0$  in finite time. Also, from (10) it follows that  $x_1 = 0$  in finite time.

#### IV. SIMULATION RESULTS

To show the effectiveness of the proposed control law, simulations are carried out on the vehicle model, the system parameters used are listed in Table II.

Parameter	Value	Parameter	Value	Parameter	Value
$m_c$	1800	$\tau$	0.0043	$C_d$	0.65
$m_w$	50	$J$	18.9	$\rho$	1.225
$A_f$	6.6	$k_b$	100	$v_w$	-6
$b_b$	0.08	$g$	9.81	$r$	0.35
$\nu$	0.95	-	-	-	-

TABLE II  
VALUES OF THE SYSTEM PARAMETERS (MKS UNITS).

To expose the performance, the proposed controllers are simulated in iced road conditions. The numerical integration was carried by applying the Euler method with a step time of  $10^{-3}$  s. The parameters for this case are given in Table I. For the proposed SM controller, the parameters used in the control law for the brake are  $\alpha = 30$ ,  $\beta = 0.001$ ,  $k_1 = 70$ ,  $k_{11} = 10$ ,  $k_{12} = 50$  and  $k_2 = 100$ .

In order to increase the longitudinal friction force, it is supposed that slip tracks a constant signal  $s^* = 0.2$ . In Figure 3 it can be seen that the selected reference  $s^*$  produces a value close to the maximum of the function  $\phi(s)$  in every road condition.

On the other hand, to show robustness property of the control algorithm in presence of parametric variations we introduce a change of the friction coefficient  $\nu$  which produces different contact forces, namely  $F(s)$  and  $f(s)$ . Then,  $\nu = 0.8$  for  $t < 10$  s,  $\nu = 0.95$  for  $t \in [10, 25)$  s, and  $\nu = 0.9$  for  $t \geq 25$  s. It is worth mentioning that just the nominal values were considered in the control design.

The figure 4 shows the wheel speed  $x_1$ . The figure 5 presents the longitudinal speed  $x_3$ . The brake controller should be turned off when the longitudinal speed is close to zero.

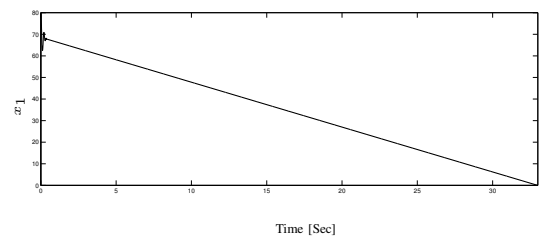


Fig. 4. Wheel velocity  $x_1$

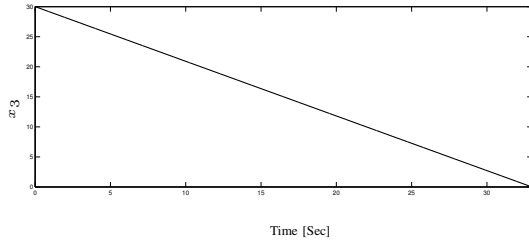


Fig. 5. Vehicle velocity  $x_3$

The figures 6 and 7 shows the tracking error  $e_1$  for the slip and the error  $e_2$  respectively.

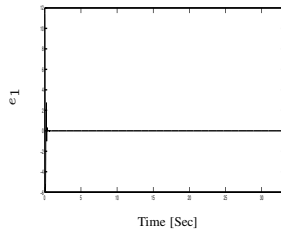


Fig. 6. Tracking error  $e_1$

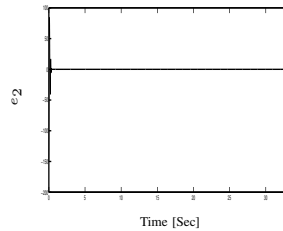


Fig. 7. Error  $e_2$

The control signal  $u$  response for the brake is presented in Figure 8.

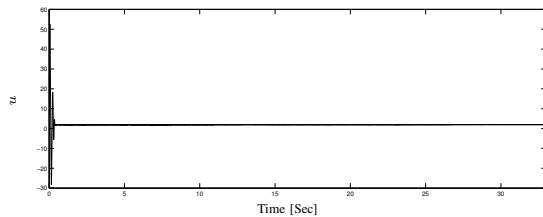


Fig. 8. Control signal  $u$

## V. CONCLUSIONS

In this work a robust control scheme was designed for the brake systems using integral SM control technique combined with quasi-continuous SM algorithms. The controller uses the SM control for achieve the error tracking asymptotically to a zero and the integral SM guarantees the disturbance rejection. The simulation results show good performance.

## REFERENCES

- Adhami-Mirhosseini, A. and M. J. Yazdanpanah (2005). Robust tracking of perturbed nonlinear systems by nested sliding mode control. In: *Proc. Int. Conf. Control and Automation ICCA '05*. Vol. 1. pp. 44–48.
- Bakker, E., H. Pacejka and L. Lidner (1989). A new tire model with application in vehicle dynamic studies. *SAE Paper No. 890087* **01**, 101–113.
- Bakker, E., L. Nyborg and H. Pacejka (1987). Tyre modelling for use in vehicle dynamic studies. *SAE Technical Paper 870421* **01**, –.
- Burton, David, Amanda Delaney, Stuart Newstead, David Logan and Brian Fildes (2004). Effectiveness of abs and vehicle stability control systems. Technical report. Royal Automobile Club of Victoria (RACV) Ltd.
- Chin, Yuen-Kwok, William C. Lin, David M. Sidlosky, David S. Rule and Mark S. Sparschu (1992). Sliding-mode abs wheel-slip control. In: *American Control Conference*. pp. 1–8.
- Clover, C.L. and J.E. Bernard (1998). Longitudinal tire dynamics. *Vehicle System Dynamics* **29**, 231–259.
- Delprat, S. and A. Ferreira de Loza (2011). Hybrid vehicle stability system using a HOSM control. In: *Decision and Control and European Control Conference (CDC-ECC), 2011 50th IEEE Conference on*. pp. 8255–8260.
- Drakunov, S. V. and V. I. Utkin (1992). Sliding mode control in dynamic systems. *International Journal of Control* **55**, 1029–1037.
- Drakunov, S. V., U. Ozguner, P. Dix and B. Ashrafi (1995). ABS control using optimum search via sliding modes. *IEEE Transactions on Control Systems Technology* **3**(1), 79–85.
- Emig, R., H. Goebels and H. J. Schramm (1990). Antilock braking systems (ABS) for commercial vehicles - status 1990 and future prospects. In: *Proc. Int Transportation Electronics Congress Vehicle Electronics in the 90's*. pp. 515–523.
- Estrada, A. and L.M. Fridman (2010). Integral hosm semiglobal controller for finite-time exact compensation of unmatched perturbations. *Automatic Control, IEEE Transactions on* **55**(11), 2645–2649.
- Huerta-Avila, H., A.G. Loukianov and J.M. Canedo (2007). Nested integral sliding modes of large scale power system.. In: *Decision and Control, 2007 46th IEEE Conference on*. pp. 1993–1998.
- Kruchinin, P.A., M. Magomedov and I.V. Novozhilov (2001). Mathematical model of an automobile wheel for antilock modes of motion.. *Mechanics of Solids* **36**(6), 52–57.
- Levant, A. (1993). Sliding order and sliding accuracy in sliding mode control. *International Journal of Control* **58**(6), 1247–1263.
- Levant, A. (2005). Quasi-continuous high-order sliding-mode controllers. *Automatic Control, IEEE Transactions on* **50**(11), 1812–1816.
- Loukianov, A. G. (2002). Robust block decomposition sliding mode control design. *Mathematical Problems in Engineering* **8**(4-5), 349–365.
- Ming-Chin, Wu and Shih Ming-Chang (2003). Simulated and experimental study of hydraulic anti-lock braking system using sliding-mode PWM control. *Mechatronics* **13**, 331–351.
- Moreno, J. A. and M. Osorio (2008). A Lyapunov approach to second-order sliding mode controllers and observers. In: *Proc. 47th IEEE Conf. Decision and Control CDC 2008*. pp. 2856–2861.
- Pacejka, H. B. (1981). In-plane and out-of-plane dynamics of pneumatic tyres. *Vehicle System Dynamics* **8**(4-5), 221–251.
- Pacejka, H. B. (2012). *Tire and Vehicle Dynamics*. Elsevier Science.
- Petrov, M.A., V.D. Balankin and O.I. Naruzhnyi (1977). Study of automobiles brakes and pneumatic tires work. model of the work process of antiblock brake system. Technical report. Novosibirsk, NISI. (In Russian).
- Rajamani, Rajesh (2011). *Vehicle Dynamics and Control (Mechanical Engineering Series)*. 2nd ed.. Springer.
- Rittmannsberger, N. (1988). Antilock braking system and traction control. In: *Proc. Int. Congress Transportation Electronics Convergence* **88**. pp. 195–202.
- Sánchez-Torres, Juan Diego, Alexander G. Loukianov, Marcos I. Galicia and Jorge Rivera Domínguez (2013). Robust nested sliding mode integral control for anti-lock brake system. *Int. J. of Vehicle Design* **62**(2/3/4), 188–205.
- Tan, H.S. and Y.K. Chin (1991). Vehicle traction control: variable structure control approach. *Journal of Dynamic Systems, measurement and Control* **113**, 223–230.
- Tanelli, M., C. Vecchio, M. Corno, A. Ferrara and S.M. Savaresi (2009). Traction control for ride-by-wire sport motorcycles: A second-order sliding mode approach. *Industrial Electronics, IEEE Transactions on* **56**(9), 3347–3356.
- Tunay, I. (2001). Antiskid control for aircraft via extremum-seeking. In: *American Control Conference, 2001. Proceedings of the 2001*. Vol. 2. pp. 665–670.
- Unsal, C. and K. Pushkin (1999). Sliding mode measurement feedback control for antilock braking systems. *IEEE Transactions on Control Systems Technology* **7**(2), 271–278.
- Utkin, V. I. (1992). *Sliding Modes in Control and Optimization*. Springer Verlag.
- Utkin, V. I., J. Guldner and J. Shi (2009). *Sliding Mode Control in Electro-Mechanical Systems, Second Edition (Automation and Control Engineering)*. 2 ed.. CRC Press.